PDMS (Polydimethylsiloxane) Microfluidic Chip Molding for Love Wave Biosensor

H. Tarbague[a], J.-L. Lachaud[a], S. Destor[a], L. Vellutini[b], J.-P. Pillot[b], B. Bennetau[b], E. Pascal[c], D. Moynet[c], D. Mossalayi[c], D. Rebière[a], C. Dejous[a]

[a] Université de Bordeaux, IMS, ENSEIRB, CNRS UMR 5218, Talence 33405, France
[b] Université de Bordeaux, ISM, CNRS UMR 5255, Talence 33405, France
[c] Université de Bordeaux, Laboratoire d'Immunologie et Parasitologie, Bordeaux 33076, France

ABSTRACT

We present the development of new Polydimethylsiloxane (PDMS) chips, which are coupled with Love acoustic wave sensors to realize a detection cell of bio-organisms in liquid media. Three generations of biocompatible PDMS chips have been developed. Built-in thermistors allow a thermal control (±0.05°C). Unlike the usual assemblies, this chip is maintained by pressure on the sensor and not sticked on its surface. This technique makes it entirely removable and cleanable. Therefore, the surface of the sensor can be functionalized or regenerated. The realization of these chips is quick and inexpensive. We here outline the development of these different cells and present characteristics of the resulting microsensors, depending on the chip configuration. Real-time responses during antibodies immobilization are presented and analyzed. Antibodies at typical concentration of 45µg/ml are successfully fast detected, with response times from 350s for static down to 90s for dynamic detection setup, with similar sensitivity. Discussions on the mechanical fluid behaviour at the near sensor surface allow to better understand these results and to investigate further developments aiming at improving the quality of the fluid stream in order to even increase future sensor characteristics.

Index Terms: Biosensors, microfluidics, PDMS, Love wave, SAW

1. INTRODUCTION

Surface acoustic wave (SAW) sensors, based on piezoelectric effect, are used in many areas since decades. In 1885, Lord Rayleigh introduced the description of the SAW and predicted its properties. Rayleigh waves have longitudinal and vertical shear components that can couple with any media in contact with the surface. This coupling strongly affects the amplitude and velocity of the wave, allowing SAW sensors to directly sense mass and mechanical properties. Their technology is based on several piezoelectric substrate materials, depending of the application areas and the needed sensitivity: quartz (SiO_2), lithium tantalate ($LiTaO_3$), lithium niobate ($LiNbO_3$), gallium arsenide (GaAs), silicon carbide (SiC), langasite (LGS), zinc oxide (ZnO), aluminum nitride (AlN), lead zirconium titanate (PZT), polyvinylidene fluoride (PVdF). Quartz substrate is the most common because the process used for manufacturing is well-known, furthermore, choosing the cut angle and the wave propagation direction, allows to adapt the temperature dependence of the material and the nature of wave polarization for a specific application. Due to their simplicity, size, high resistance, high sensitivity, versatility, SAW sensors are integrated in a lot of devices in many areas of sensing: pressure [1], chemical [2], vapor [3], humidity [4], temperature [5], mass sensors [6], telecommunications [7], biosensors [8], rheology and seismology [9].

In this context we use SAW sensors based on guided shear horizontal surface acoustic waves (guided SH-SAW) or Love waves, predicted by A.E.H Love in 1911, for detection in liquid media thanks to their great surface sensitivity to mass loading effect and ability to work with adjacent liquid thanks to SH polarization.

Recently, the advent of microfluidic systems, introduced by pioneer groups in this area, like The George Whitesides Research Group [10-12], revolutioned the biosensing world. Since it, the development of PDMS chips for microfluidics has known an extraordinary expansion. Nowadays, such devices offer a new approach in many areas, such as biology,

medicine, chemistry, crystallography or optical [13-17]. The laboratories involved in medical analyses and chemical industries are interested in these promising technologies for Lab-On-Chip development, where all analyses could be performed in few cubic centimetres, diminishing expenses in a prodigious way.

For most of these devices, PDMS is the raw matter. In recent years, siloxane-based elastomers such as PDMS have been heavily exploited in microtechnology, since they are non-toxic, biocompatible and commercially available.

As a consequence, microfluidic approach has been investigated with various biotransducing microtechnologies, for examples : surface plasmon resonance (SPR) [18], optical transducers based on absorbance [19] or chemiluminescence [20] and thermal transducers [21]. Microfluidic biosensors based on electrochemical detection have also been investigated [22], as well as acoustic technologies such as Quartz Crystal Microbalance [23].

In this context, SAW sensors are ideal candidates for the development and coupling with microfluidic devices, in which, at term, all components will be integrated. Recent developments with such sensors allowed the study of low volumes of liquid (µl) [24], with applications such as microrheometer to probe in real-time the high frequency behaviour of liquids with a wide spectrum of viscosity. For biosensing aims, their surface can be functionalized and they can potentially detect specifically with particularly great sensitivity a large number of molecules or species investigated.

In this paper, we present the development of new PDMS chips coupled with Love acoustic wave sensors to realize a detection cell for microorganisms. We shall expose first the characteristics of the sensor and materials used. Then, an original prototyping technology for polymeric 3D-cells molding will be presented, as well as its use for the development of PDMS chips with different architectures, allowing hydrostatic and hydrodynamic configurations. Compared to other studied devices associating SAW and PDMS analyte chambers, a particular effort has been paid to the ability to remove the PDMS cell, which is not sticked on the sensor surface, but rather maintained by pressure on it. A part is then devoted to experimental results: electrical characteristics, depending on the chip configuration and with saline biological buffer solution, and antibodies grafting biodetection. These results are finally discussed, their interpretation is mainly based on mechanical considerations about the fluid motions at the near sensor surface. This allows us to initiate further improvements to enhance the sensors characterictics.

As presented, the system is very adaptive and potentially allows the study of rheological properties of a large variety of liquids. It is possible to detect a large number of biological species, by designing specific functionalization layer. The system is completely removable, the PDMS cells are chemically inert, biocompatible, cleanable and reusable. They can be made hydrophilic or hydrophobic, depending on the application. This technique is simple to implement and generates few pollutants.

2. MATERIALS AND METHODS

A. Love Wave Sensor

The Love wave sensor is a multilayered structure composed of a quartz substrate, titanium/gold interdigital transducers (IDTs) and a SiO2 guiding layer. This acoustic sensor is based on a piezoelectric delay-line, with a transmitter and a receiver consisting of metallic (IDTs) to generate and detect an acoustic wave by inverse piezoelectric effect (Fig.1).

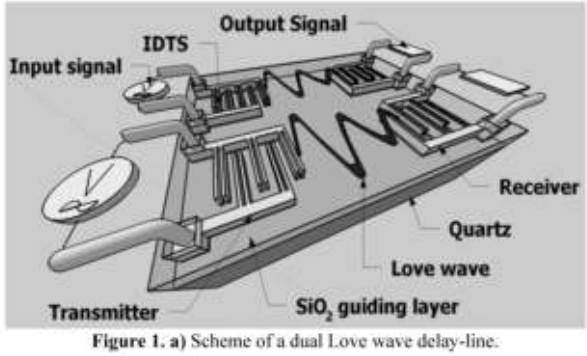

Figure 1. a) Scheme of a dual Love wave delay-line.

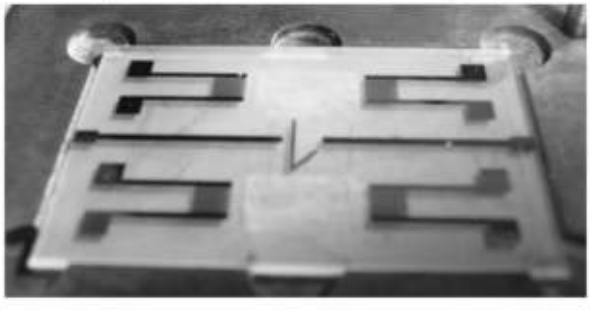

b) Photo of a dual Love wave delay-line.

An AT-cut quartz substrate with IDTs orientation cho-sen to allow a wave propagation perpendicular to X crystallographic axis (Euler Angles: 0°; 121.5°; 90°), permits to generate pure shear horizontal (SH) waves, and so to work in an adjacent liquid medium. The IDTs (typically 700 nm gold on a 400 nm titanium layer) have been processed using lift-off technique. A 4 µm SiO_2 guiding layer was obtained via plasma enhanced chemical vapor deposition (PECVD) to trap acoustic energy within the SiO_2 to generate guided SH-SAW (Love wave). Finally, the SiO_2 was etched upon electrical contacts. More details on the acoustic delay-

lines design and process can be found in previous reports, for example in [25]. These parameters lead to a synchronous frequency of about 115 MHz and -30 dB of insertion losses (S21 scattering parameter). Note that for all electrical characterization using network analyzer or oscillating configuration for detection tests, the delay-lines were used in differential mode with baluns (radiofrequency transformers) to avoid common mode especially for liquid applications.

Furthermore, each sensor was composed of two delay-lines in order to perform differential measurements, with one acting as a reference signal, or for dual measurement with further aim of parallelization.

A PDMS chip is placed on the device to control microcavities delimiting the fluid on the sensor surface.

A test cell derived from that described in [26] allowed to maintain homogeneous and quite reproducible pressure on the PDMS chips above the acoustic wave microsensor, ensuring water tightness of the analyze chamber.

B. GPTS functionalization of the SAW sensor surface for biodetection.

The antibodies were bonded onto the SiO_2 surface using a GPTS monomolecular film [27].

The sensitive layer ideal configuration would be to densely immobilize antibodies onto the whole sensor surface by the crystallisable fragment (Fc) and let the antigen binding site free for antigen binding, but GPTS does not favour any antibody orientation. The sensor surface was first washed in an ethanol solution with ultrasounds and then cleaned with UV-O_3. The GPTS molecule (1% in toluene) was grafted under acidic condition (acetic acid, 19% in molar concentration) to functionalize the sensor surface; GPTS was covalently bonded to SiO_2 substrates (Fig. 2) by reaction between the silanol groups of the surface and hydrolysed alkoxysilane moieties, so constituting an epoxy silylated monomolecular film on the Love wave device.

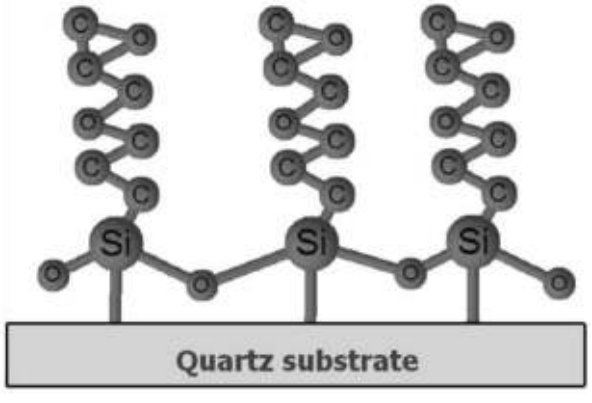

Figure 2. Schematic representation of SiO_2 surface silanized with GPTS.

Then the antibodies could be covalently linked to this modified surface by reaction between the epoxy group of GPTS and the amino groups of antibodies.

C. Biological material

The biological material used was starting block™ blocking buffer (SBBB) (Pierce, ref 37538), goat anti-mouse IgG (whole molecule)-peroxidase antibodies (GAM) (Sigma–Aldrich, ref A4416), anti-bacteriophage monoclonal antibodies (Amersham Biosciences, anti-M13 monoclonal antibodies, ref 27-9420-01). All antibodies were suspended in triphosphate buffered saline (TBS), pH 7.2, 0.15M.

D. Acquisition loop.

The sensor test cell was composed of the PDMS chip (including two analyte chambers) pressed on the sensor. Placed in a thermoregulated system to control the sensor temperature, this platform was inserted in an oscillation loop to provide a frequency output signal real time monitored (12 bit frequency counter, Agilent 51131A) with thermostated oscillator. The working temperature could be measured with a platinum resistance thermometer (Pt100) embedded in the PDMS against the analyze chamber during the chip molding. A heating resistor screenprinted on a ceramic placed under the SAW sensor allowed a thermal control (±0.05°C). The Pt100 measured the temperature and transmitted this information to a proportional–integral controller (PI controller), programmed with a PIC 16F 874 microcontroller (Microchip ©), which controlled the heating power supplied to the heating ceramic through an internal PWM (pulse width modulation) module.

The signals from the frequency counter and the multimeter were computer monitored. A LabWindows™/CVI™-based software was developed to process experimental datas (one measurement every second), and displayed the frequency shifts of delay-lines as a function of time.

Liquid handling was achieved with a Bioseb BS800 programmable syringe pump via Hamilton glass syringes and PTFE capillary tubes connected to the inlet/outlet channels of the PDMS chips.

3. 3D-PDMS CHIPS MOLDING

A. Introduction

Three types of home-made micro-machined aluminum molds were designed for rapid polymer prototyping, allowing three generations of PDMS 3D-chip architectures, with pre-cut calibrated shapes,

which is essential for a good repeatability of the tests conditions (temperature, pressure). This process of manufacturing had been chosen for the preparation of PDMS chips due to its great versatility to realize prototypes, with other advantages such as using no polluting materials. Aluminum was selected as mold basic material due to its weak affinity towards PDMS and ease to manufacture. These molds were designed using SketchUp Pro 3D sketching software, then conveniently exported in dxf format, directly used in the interface program of computer controlled micro-milling machine robot.

The first mold allowed to realize PDMS chips for a first « diffusion » setup or hydrostatic setup (HSSU1), consisting in getting the fluid sample in, then out, of the open analyze chamber with a micropipette. On the first hydrostatic chip (HSSU1), the fluid sample covers the entire acoustic path, as well as above IDTs (electrically isolated from the liquid by the SiO_2 guiding layer).

The second mold was used for a second « diffusion » setup (HSSU2). The HSSU2 was characterized by emitting and receiving areas isolated from the liquid by air cavities, separated from the analysis chamber by PDMS walls of 250 µm. In these static configurations, the sensor surface remains entirely accessible and the fluid sample does not move above the sensor after injection with a micropipette.

In order to improve the control of the microfluidic flow on the sensor surface, a third mold with different patterns and enhanced prototyping technology was designed. This third mold allowed to achieve a hydrodynamic setup (HDSU), consisting in flowing the fluid with a programmable syringe pump through microchannels above the microsensor. As in HSSU2, emitting and receiving areas are isolated from the liquid by air cavities, separated from the analysis chamber by PDMS walls (250 µm).

B. HSSU1

The first mold (figure 3), used for the hydrostatic setup 1 (HSSU1), is composed of three elements: the basis, the middle and the cover parts.

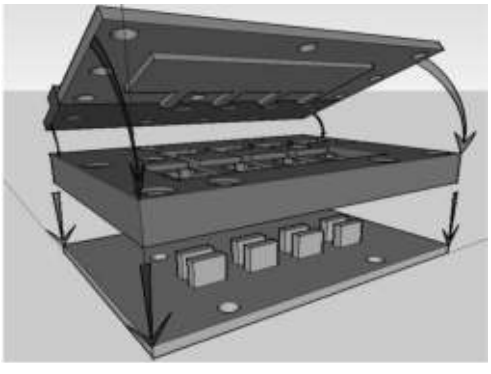

Figure 3. Scheme of the three parts aluminum mold for HSSU1.

On the basis, four same shapes are machined and used as negatives delimiting the internal dimensions of the fluid chambers. The middle part of the mold delimits the external shapes of the cells and the cover allows to calibrate their height. The two components of PDMS kit (Dow Corning, Sylgard 184 silicone elastomer) are thoroughly mixed (base/curing agent: 1/9 by weigh, placed under vaccum to remove entrapped air during one hour, and poured in the aluminum container (base and middle assembled parts). The cover is then placed and PDMS in excess is channeled and retained by the exhaust chambers in the cover. Entrapped air is removed again during 1h30 under vacuum. Then the silicone is heat cured by placing the mold on a hot plate at 95°C for 20 minutes. Finally, the mold is dismantled to recover the PDMS cells. All these preparation steps are recapitulated on the table I, the entire process duration is 3h15.

Table I. Steps of the PDMS chip molding and their duration.

HSSU mold	
Steps	Duration (min)
PDMS mixing	15
PDMS deairing	60
PDMS dispensing	15
Post deairing	90
Heat curing	20
Total time	195

These PDMS chips offer several interesting characteristics: besides their biocompatibility, they are calibrated in height with an accuracy of 10 µm to facilitate reproducible pressure assembly on the microsensor. Henceforth, these cells allow to have a completely removable device and thus make possible the cleaning and reuse of SAW sensors. The so-obtained HSSU1 experimental apparatus chip is represented on figure 4.

C. HSSU2

The second mold, used for the hydrostatic setup 2 (HSSU2), is quite similar to the previous one. The main difference is the analyte chamber length which is shortened to let thin air cavities upon IDTs, with a negative shape as represented on figure 5.

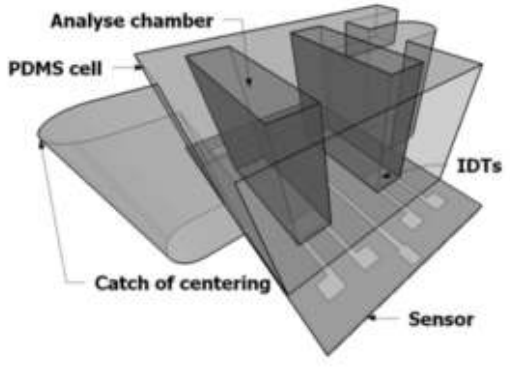

Figure 4. HSSU1 Chip.

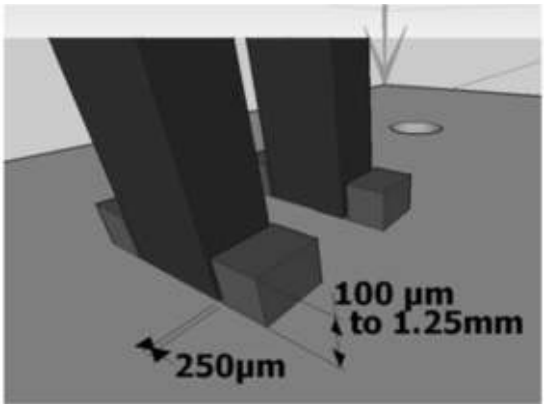

Figure 5. Dimensions of the pads of the base for the HSSU2 mold.

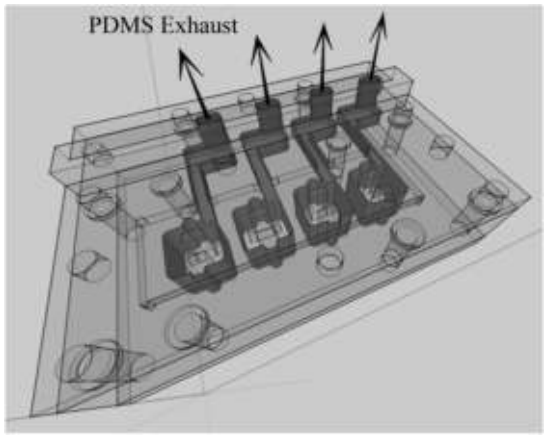

Figure 6. Chip shape with the HSSU2 mold.

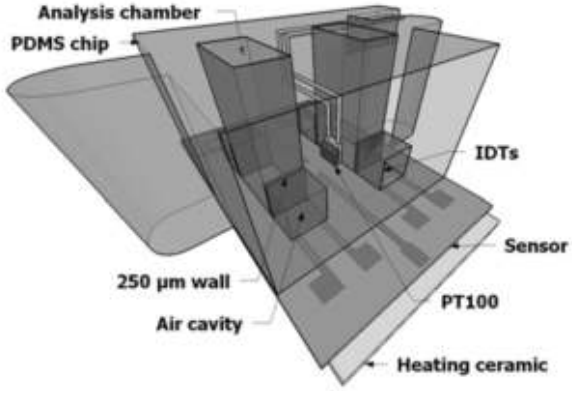

Figure 7. HSSU2 Chip.

Another major difference is the fabrication process, as indicated in Table 2. In this case, the PDMS is molded to make first the air cavities. The first heat curing allows to create a seal between the base and the middle parts, facilitating deairing in the second step (statement below). A second solution of mixed and deaired PDMS is poured in the container to completely fill up the cavities. The cover is then placed and PDMS in excess is channeled and retained by the openings in the cover. The second deairing step needs to be longer (2 hours under vacuum), as the PDMS has begun to reticulate and it is difficult to remove the remaining entrapped air. The silicone is then heat cured again and the mold is dismantled to recover the PDMS cells. All the preparation steps are recapitulated on the table II, showing a total preparation duration as long as 6h.

The mold and the so-obtained HSSU2 experimental apparatus chip are represented on figures 6 and 7.

Note that an embedded thermistor (Pt100) has been represented: it was placed just after the first mold deairing and encapsulated during the first mold heating.

D. HDSU

Both previous molds and architectures aimed at validating the new concept of "free" cells, maintained by pressure on the sensor surface, together with keeping chambers with quite high volume, necessary in some applications to have representative analyte samples. For many other applications, on the contrary, it will be interesting to lower the samples volumes. Furthermore, the diffusion movements in both HSSU architectures is obviously non efficient to favor the presence of target species at the near surface of the sensor, limiting their immobilization and as a consequence the overall sensor sensitivity.

Table II. steps of the PDMS chip molding and their time.

HSSU mold	
Steps	Time in minutes
First PDMS mixing	10
First PDMS deairing	60
First PDMS dispensing	15
First mold deairing	30
First mold heating	20
Second PDMS mixing	10
Second PDMS deairing	60
Second PDMS dispensing	15
Mold deairing	120
Mold Heating	20
Total time	360

This third mold aims to introduce a hydrodynamic configuration, both with lower chambers volumes and with controlled microfluidic stream. This mold for a hydrodynamic setup (HDSU) is composed of four elements (figure 8): the basis, a viton join, the middle and the cover parts.

In this mold, the four parts are assembled first, and then the PDMS mixed preparation is injected with a syringe pump. The viton join between the base and the middle parts avoids PDMS outflow when injected under pressure. As for the HSSU2 mold, the HDSU mold with PDMS was cured on a hot plate at 95°C for 20 minutes and dismantled to recover the PDMS cells.

Compared with the HSSU2 mold, the time required to achieve chips with the HDSU mold is drastically reduced, as air entrapment is always almost eliminated due to syringe injection.

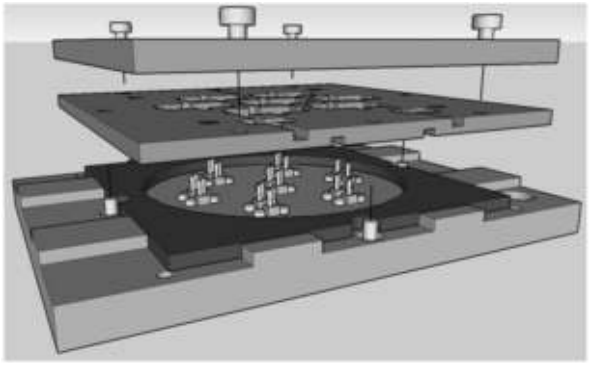

Figure 8. Scheme of the four parts aluminum mold.

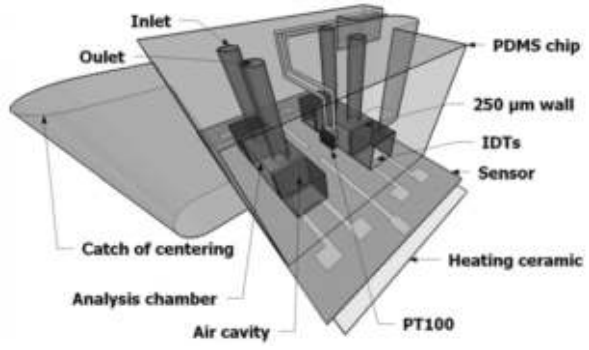

Figure 9. HDSU2 Chip.

The so-obtained HDSU experimental apparatus chip is represented on figure 9. Two heights of analyte chambers were realized: 100 µm and 1.25 mm (respective volumes: 1,5 µl for HDSU1 and 18.5 µl for HDSU2). Access holes were directly integrated in the mold pattern. In this dynamic mode, the liquid sample is confined near the sensor surface and flows along with the acoustic path, on the main sensitive part of the microsensor, therefore favorizing species renewal on the biorecepting layer.

For this hydrodynamic setup, pipettor cones were inserted in the inlet channels of the PDMS chip. These cones were the primary tanks for the liquid samples, their use avoided trapping air bubbles in the analyze chamber during the acquisition and mechanical shocks. Air bubbles and mechanical shocks must be avoided because they can generate frequency jumps, similar but not related to a detection

4. RESULTS

A. Insertion losses

The electrical characteristics were measured with a network analyser (ANRITSU, SCORPION MS4623B, Morgan Hill, CA). Typical insertion losses (S21 scattering parameters) versus the frequency are reported on figure 10.

On this figure, the characteristic of the bare delay-line (without PDMS chip, under air, curve a.) highlights

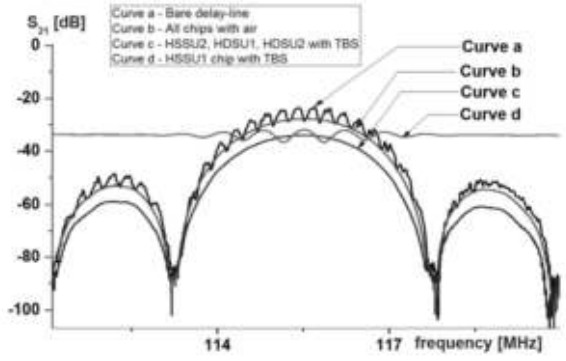

Figure 10. Insertion losses of the SAW-PDMS chips.

a synchronous frequency near 115.6 MHz (associated with 40 µm IDTs spatial periodicity) and acoustic reflections on the sensor edges (IDTs are bidirectional).

With the first HSSU chip under air (curve b.), these parasitic reflections are trapped in the elastomeric material and they are so eliminated. The characteristics with the HSSU2 and HDSU chips with air are very similar to that obtained on curve b.

However, when saline biological buffer solution (triphosphate buffer solution - TBS) is injected in this HSSU1 cell, the acoustic wave energy almost disappears (curve d.), due to an electromagnetic (EM) signal which is visible and can be isolated in the time domain (curve not shown). This EM signal is induced by parasitic capacitance between IDTs and conducting liquid above them, even in differential mode, with baluns on both ports of the delay-line.

Air cavities encapsulating IDTs, for example with the second HSSU chip (curve c.), allows to eliminate this EM signal, and so to recover the acoustic energy with a good rejection level with respect to side lobes and to the noise floor. As previously, the PDMS outside walls absorb unwanted acoustic reflections.

The delay-lines with HDSU chip have been tested in the dynamic mode, with fluid (TBS) flowing through the analysis chamber. Their characteristics have shown no difference compared to that represented on curve c (delay-line with the second chip, with TBS in static mode), even when changing the flow parameters: pumping the fluid in or out the analysis chamber, at flow rates from 1 µL/min to 20 mL/min for the HDSU chips. These flow rates correspond to renewal of the

Table III. Rate of flow and average speed laminar flow.

	Flowrate in µl/min	Liquid speed in µm/s
HDSU1	1	560.10^{-3}
	25	14
	250	139
	25.10^{3}	$13,9.10^{3}$
HDSU2	10	440.10^{-3}
	25	***1***
	250	11
	25.10^{3}	$1,1.10^{3}$

TBS in the chamber up to 240 times per second (mean value of the speed of the laminar flow in table III).

Same results were obtained with deionized water instead of TBS, with colored ink to visually control the cell watertightness, either in static or dynamic mode (HSSU2 and HDSU). Finally, it was observed that watertightness could be improved by rinsing the chips with ethanol and acetone after each use, and by exposing their bottom surface to UV-ozone cleaner during 180 seconds before placing them on the microsensor surface. This last step allows to promote "soft" adhesion on the substrate.

B. Gam-g Antibodies detection

The different setup were used with the same sample volume of 250µl to compare the kinetics of bioreceptors immobilization. For both HDSU, an empirically optimized flow rate of 25 µl/min was used.

The sensor responses with HSSU2 and both HDSU chip configurations were compared during grafting of Goat Anti-Mouse antibodies (GAM-γ, 40 µg/ml). Antibodies real-time detection curves are represented on figure 11.

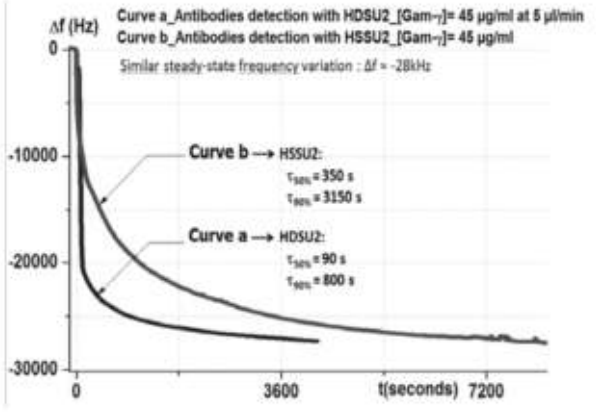

Figure 11. Antibodies grafting responses with the HSSU2 and the HDSU2.

It can be observed similar steady-state frequency variations: 28 kHz with the HSSU2 and the HDSU2, validating similar efficiency to immobilize antibodies with both setup. But the response time is highly different. Indeed, it can be seen from Figure 11 and Table IV that the steady-state frequency shift detection time is divided by four with the HDSU2, with a typical $\tau_{90\%}$ reduced to only a couple of minutes.

Table IV. Typical response times for GAM-g grafting (250 ml, 40 mg/ml, 25 ml/min).

	$\tau_{50\%}$ (s)	$\tau_{90\%}$ (s)
HSSU2	350	3250
HDSU	90	800

These differences were attributed to the better fluid confinment and renewal near the sensor surface, whereas a fluid boundary layer can be assumed in higher cavities, and even more in open chamber, limiting diffusion of biological species towards the reactive surface.

5. DISCUSSION

In order to support these results and their analyze, concerning the efficiency of the liquid flow in the analyze chamber, several cell types with different shape ratio geometries were pressed on a glass slide. A numeric camcorder was placed under the system to real-time visualize the streams, by using fluids of different colors flowing alternatively in the chamber. Resulting videos let to observe two zones. In the first zone, close to the sensor surface, the fluid, governed by diffusion, moves very slowly. In the second zone, governed by laminar flow, it moves more rapidly. For example, with a flow rate theoreticcaly allowing complete renewal of the volume 10 times per second, when the color liquid is changed, it takes almost as high as 5 minutes to change the color at the near surface. Velocity gradients (i.e concentrations) are observed.

Despite the slow movement of the fluid on the sensor surface, and the inhomogeneous distribution of the antibodies on its surface, it is sufficient to significantly reduce the antibodies response time. However, the steady-state frequency shifts were similar with both configurations (HSSU2 and HDSU2), provided that antibodies were in large excess to saturate the sensor surface in both cases.

To explain these results, it is important to consider them from a mechanical point of view: the average travel time of a particle in diffusive regime is much important that the average travel time of a particle in a laminar flow. The sensor response is directly linked to the mass attached on its surface. It is therefore essential to graft lots of antibodies in a short time on the sensor surface. Consequently, the diffusive regime, close to the sensor, must be replaced by an advective regime.

For this reason an efficient microfluidic approach of the problem is necessary to control the liquid flow stream near the sensor surface. With this purpose, new microfluidic networks are under development. These microfluidic networks will include mixers aiming to homogenize the flow and the antibodies distribution on the sensor surface, reducing the velocity gradient in the analyze chamber. With a height of several tens of micrometers to confine the liquid media to the sensor surface, a final objective is to increase the graft rate of the antibodies, thus improving both detection time and sensitivity, and consequently improving also the detection threshold.

These microfluidic networks will also permit to reduce the quantities of biological materials, which is particularly interesting when using expensive antibodies.

6. CONCLUSION

A thermo-regulated Love acoustic wave platform for biosensing applications was realized. We have shown the feasibility of a microsensor for use in liquid medium, based on the association of a SAW sensor and a removable PDMS chip. Different architectures of the PDMS chip have been studied. They have been characterized with various fluids and flow protocols, in hydrostatic or hydrodynamic regime. The validity of this approach to detect chemical molecules or biological micro-organisms has been demonstrated. New hydrodynamical PDMS chips integrating microfluidic flow, associated with acoustic Love wave sensors, have led to high-speed micro-organisms detection, with efficient antibodies detection in less than two minutes.

Further studies aim at developing even more efficient microfluidic cavities, integrating geometrical specificities in order to favor an advective regime improving interactions and their kinetics at the near sensor surface. Combining this device with microfluidic mixers and microfluidic pumps should allow to realize portative µTAS (micro total chemical analysis system) for biodetection and bioanalysis in various liquid media.

ACKNOWLEDGMENTS

The works were realized in the frame of a project of the Agence Nationale de la Recherche (ANR-06-ECOT-004). The authors also would like to thank Véronique Conédéra and Monique Benoît from LAAS-CNRS (Toulouse - France) for acoustic delay-lines technological realization, as well as Matthieu Guirardel from Laboratoire du Futur (CNRS UMR 5258) and Vincent Raimbault for valuable scientific discussions on PDMS technical realizations.

REFERENCES

[1] W. Wang, K. Lee, I. Woo, I. Park, S. Yang, Optimal design on SAW sensor for wireless pressure measurement based on reflective delay-line, Sensors and Actuators A: Physical, Volume 139, Issues 1-2, 12 September 2007, Pages 2-6.

[2] B.Joo, J.S. Huh, D.D. Lee, Fabrication of polymer SAW sensor array to classify chemical warfare agents, Sensors and Actuators B: Chemical, Volume 121, Issue 1, 30 January 2007, Pages 47-53.

[3] Y. Zhao, M. Liu, D-M. Li, J-J. Li, J-B Niu FEM modeling of SAW organic vapor sensors , Sensors and Actuators A: Physical, Volume 154, Issue 1, 31 August 2009, Pages 30-34.

[4] M. Penza, V. I. Anisimkin, Surface acoustic wave humidity sensor using polyvinyl-alcohol film, Sensors and Actuators A: Physical, Volume 76, Issues 1-3, 30 August 1999, Pages 162-166.

[5] R. Fachberger, A. Erlacher, Monitoring of the temperature inside a lining of a metallurgical vessel using a SAW temperature sensor Procedia Chemistry, Volume 1, Issue 1, September 2009, Pages 1239-1242.

[6] R.D.S. Yadava, Enhancing mass sensitivity of SAW delay-line sensors by chirping transducers, Sensors and Actuators B: Chemical, Volume 114, Issue 1, 30 March 2006, Pages 127-131.

[7] Q. Fu, H. Stab, W. Fischer, Wireless passive SAW sensors using single-electrode-type IDT structures as programmable reflectors , Sensors and Actuators A: Physical, Volume 122, Issue 2, 26 August 2005, Pages 203-208.

[8] K. Länge and M. Rapp, Influence of intermediate hydrogel layer and amount of binding sites on the signal response of surface acoustic wave biosensors, Sensors and Actuators B: Chemical, Volume 142, Issue 1, 12 October 2009, Pages 39-43.

[9] V.V. Ruzhich, S.G. Psakhie, E.N. Chernykh, S.A. Bornyakov, N.G. Granin, Deformation and seismic effects in the ice cover of Lake Baikal, Russian Geology and Geophysics, Volume 50, Issue 3, March 2009, Pages 214-221.

[10] A.D. Stroock, S.K.W. Dertinger, A. Ajdari, I. Mezic, H.A. Stone et G.M. Whitesides : Chaotic mixer for microchannels. Science, 295, January 2002, Pages 647–651.

[11] Y. Xia et G. M. Whitesides : Soft lithography. Annual Review of Materials Science, 28(1), 1998, Pages 153–184.

[12] D. C. Duffy, J. C. McDonald, O. J. A. Schueller et G. M. Whitesides: Rapid prototyping of microfluidic systems in poly(dimethylsiloxane). Analytical Chemistry, 70(23), 1998, Pages 4974–4984.

[13] N. Kim, C.M. Dempsey, J.V. Zoval, JI-Y. Sze, M.J. Madou: Automated microfluidic compact disc (CD) cultivation system of Caenorhabditis elegans, Sensors and Actuators B, 122, 2007, Pages 511-518.

[14] B.T. Ginn, B. Steinbock, M. Kahveci and O. Steinbock: Microfluidic Devices for the Belousov-Zhabotinsky Reaction, J. Phys. Chem. A, 108, 2004, Pages 1325-1332.

[15] J.G. Lim, S.S. Lee, K.D. Lee: Polymeric arrayed waveguide grating using imprint method incorporating a flexible PDMS stamp, Optics Communications 272, 2007, Pages 97-101.

[16] C-H. Wang, G-B. Lee: Automatic bio-sampling chips integrated with micro-pumps and micro-valves for disease detection, Bioelectronics, 21, 2005, Pages 419-425.

[17] Kang-Yi Lien, Wan-Chi Lee, Huan-Yao Lei, Gwo-Bin Lee: Integrated reverse transcription polymerase chain reaction systems for virus detection, Biosensors and Bioelectronics 22, 2007, Pages 1739–1748.

[18] D.S. Kim, J-E. Park, J-K. Shin, P. K. Kim, G. Lim, S. Shoji. An extended gate FET-based biosensor integrated with a Si microfluidic channel for detection of protein complexes. Sensors and Actuators B: Chemical, Volume 117, Issue 2, 12 October 2006, Pages 488-494

[19] S. Demming, A. Llobera, R. Wilke, S. Büttgenbach , Single and Multiple Internal Reflection poly(dimethylsiloxane) absorbance-based biosensors, Sensors and Actuators B: Chemical, Volume 139, Issue 1, 20 May 2009, Pages 166-173.

[20] Yi Lv, Z. Zhang, Funan Chen , Chemiluminescence microfluidic system sensor on a chip for determination of glucose in human serum with immobilized reagents ,Talanta, Volume 59, Issue 3, 1 March 2003, Pages 571-576.

[21] Y. Zhang, S. Tadigadapa . Calorimetric biosensors with integrated microfluidic channels. Biosensors and Bioelectronics, Volume 19, Issue 12, 15 July 2004, Pages 1733-1743.

[22] S. Choi, J. Chae, Reusable biosensors via in situ electrochemical surface regeneration in microfluidic applications, Biosensors and Bioelectronics, Volume 25, Issue 2, 15 October 2009, Pages 527-531.

[23] B. D. Spangler, B. J. Tyler.Capture agents for a quartz crystal microbalance-continuous flow biosensor: functionalized self-assembled monolayers on gold Analytica Chimica Acta, Volume 399, Issues 1-2, 8 November 1999, Pages 51-62 .

[24] V. Raimbault, D. Rebière, C. Dejous, M. Guirardel, V. Conédéra, J. Pistré, Higt viscosity sensing using a Love wave acoustic platform combined with a PDMS microfluidic chip, ECS Transactions, 4 (1), 2006, Pages 73-81.

[25] N. Moll, E. Pascal, b, D.H. Dinh, J.-P. Pillot, B. Bennetau, D. Rebière, D. Moynet, Y. Masd, D. Mossalayi, J. Pistré, C. Déjous, A Love wave immunosensor for whole E. coli bacteria detection using an innovative two-step immobilisation approach, Biosensors and Bioelectronics 22, 2007, Pages 2145–2150.

[26] V. Raimbault, D. Rebière, C. Dejous, J. Pistré, J.-L. Lachaud, M. Guirardel, High frequency microrheological measurements of PDMS fluids using SAW microfluidic system, Sensors and Actuators B, in press (2009).

[27] D.H. Dinh, L. Vellutini, B. Bennetau, C. Dejous, D. Rebière, E. Pascal, D. Moynet, C. Belin, B. Desbat, C. Labrugère, J-P. Pillot: A Route to Smooth Silica-Based Surfaces Decorated with Novel Self-Assembled Monolayers (SAMs) Containing Glycidyl-Terminated Very Long Hydrocarbon Chains, Langmuir 2009, 25, Pages 5526-5535.